

# Interactive segmentation for geographic atrophy in retinal fundus images

Noah Lee, *IEEE Member*, R. Theodore Smith, Andrew F. Laine

**Abstract** - Fundus auto-fluorescence (FAF) imaging is a non-invasive technique for in vivo ophthalmoscopic inspection of age-related macular degeneration (AMD), the most common cause of blindness in developed countries. Geographic atrophy (GA) is an advanced form of AMD and accounts for 12-21% of severe visual loss in this disorder [3]. Automatic quantification of GA is important for determining disease progression and facilitating clinical diagnosis of AMD. The problem of automatic segmentation of pathological images still remains an unsolved problem. In this paper we leverage the watershed transform and generalized non-linear gradient operators for interactive segmentation and present an intuitive and simple approach for geographic atrophy segmentation. We compare our approach with the state of the art random walker [5] algorithm for interactive segmentation using ROC statistics. Quantitative evaluation experiments on 100 FAF images show a mean sensitivity / specificity of 98.3 / 97.7% for our approach and a mean sensitivity / specificity of 88.2 / 96.6% for the random walker algorithm.

**Index Terms** — Interactive Segmentation, Geographic Atrophy, AMD, Autofluorescence, Watershed Transform, Random Walker, ROC.

## I. INTRODUCTION

Fundus auto-fluorescence (FAF) imaging is a non-invasive technique for in vivo ophthalmoscopic inspection of age-related macular degeneration (AMD), the most common cause of legal blindness in developed countries [3]. FAF signals are reliable markers of lipofuscin in retinal pigment epithelium (RPE) cells [1, 2]. Geographic atrophy (GA) of the RPE, an advanced form of AMD, accounts for 12-21% of severe visual loss in this disorder [3].

Automatic quantification of GA is important for determining disease progression and facilitating clinical diagnosis of AMD. The problem of automatic segmentation of pathological images has been widely studied yet it still remains an unsolved problem in medical image analysis [5]. The current state of the art shows that few automated image analysis techniques can be applied fully autonomously with reliable results. Interactive segmentation schemes may be seen as an

appropriate alternative to solve the problem of robust and accurate segmentation [5, 20, 21]. Often times post-processing of the segmentation obtained is necessary to validate segmentation accuracy. In the realm of computer aided diagnosis interactive segmentation schemes are well received by physicians where the combination of human and machine intelligence can provide improved segmentation efficacy at minimal expert intervention. We justify an interactive approach by assuming that automatic approaches require post-refinement tasks that may be more labor intensive than minimal expert intervention beforehand or during the segmentation. Generally, GA quantification methods in the literature have typically relied on visual inspection of FAF images [13], which prevents quantification, or time consuming manual delineation of GA boundaries in combination with semi-automatic segmentation techniques [9]. Manual quantification of GA is time consuming and prone to inter- and intra-observer variability [13].

In this paper we present an interactive segmentation approach for geographic atrophy segmentation in retinal fundus images using the watershed transform (WT) algorithm. We choose the WT algorithm due to its well defined properties and its computational efficiency [6]. In our approach we compute non-linear gradient approximations using generalized Sobel kernels to deal with varying noise levels and multi-scale edges. To overcome the well-known over-segmentation problem in WT segmentation our approach allows the expert to guide and influence the segmentation process through interactive marker placement. We compare our approach with the state of the art random walker [5] algorithm for interactive segmentation using ROC statistics on 100 test cases.

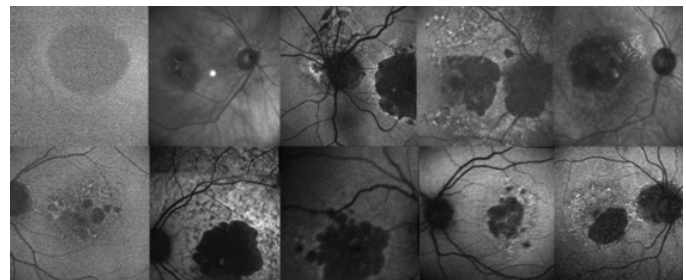


**Fig. 1.** FAF images and examples of geographic atrophy (GA). GA phenotype consists of multi-lobed atrophic patches increasing in size with clutter and occlusion. The dark areas indicate hypoauto-fluorescent GA.

Manuscript received Nov. 25, 2008. This work was supported in part by NEI (R01 EY015520), the NYC Community Trust (RTS), and unrestricted funds from Research to Prevent Blindness.

Noah Lee is with the Biomedical Engineering Department, Columbia University, New York, NY 10027 USA (phone: 212-854-5996; fax: 212-854-5995; n12168@columbia.edu).

Prof. Andrew F. Laine is with the Department of Biomedical Engineering, Columbia University, New York, NY 10027 USA (laine@columbia.edu).

Prof. R. Theodore Smith is with the Ophthalmology Department, Columbia University, New York, NY 10027 USA (rts1@columbia.edu).

GA is characterized by round or multi-lobed patches of atrophy of the RPE, the overlying retina, and the underlying choriocapillaris. Hypoauto-fluorescence is the FAF hallmark of

geographic atrophy. With atrophy of the RPE, the lipofuscin is lost and the FAF signal from that region becomes hypoauto-fluorescent or dark. Over time, atrophic patches may increase in size and number or may coalesce to form larger areas of atrophy. Imaging parameters from different institutions and inter-patient variability further cause high variability in noise, shape, texture, contrast and illumination. Figure 1 shows a subset of our example datasets of 100 FAF images.

## II. THE WATERSHED TRANSFORM

Beucher et al. first applied the concept of the watershed transform to the image segmentation problem [7] in the late 1970s. The watershed transform is a morphological segmentation technique that provides an image partitioning and found wide use in medical image processing [6]. The segmentation technique is derived directly from the topographical watershed idea whereby all points on the surface are grouped according to the concept of water falling onto the surface and flooding each local minimum until total immersion [19]. The analogy can be explained by taking the example of rain drops associated with each point in the image. Any two points are in the same region, also named a catchment basin, if they fall to the same point. The watershed lines, which divide the image, result from the catchment basins that start to meet each other as more rain falls onto the surface.

A watershed definition for the continuous case can be based on distance functions. Assume that the image  $f$  is an element of the space  $\mathcal{C}(\mathcal{D})$  of real twice continuously differentiable functions on a connected domain  $\mathcal{D}$  with only isolated critical points. Then the topographical distance between points  $p$  and  $q$  in  $\mathcal{D}$  is defined by [14]

$$T_f(p, q) = \inf_{\gamma} \int_{\gamma} \|\nabla f(\gamma(s))\| ds,$$

where the infimum is over all paths  $\gamma$  inside  $\mathcal{D}$  with  $0 = p, (1) = q$ . The topographical distance between a point  $p \in \mathcal{D}$  and a set  $A \subset \mathcal{D}$  is defined as  $T_f(p, A) = \min_{a \in A} T_f(p, a)$ . The path with shortest  $T_f$ -distance between  $p$  and  $q$  is a path of steepest slope on the graph of  $f$ . From this one can define the following definition.

**Definition 2.1. (Watershed transform)** Let  $f \in \mathcal{C}(\mathcal{D})$  have minima  $\{m_k\}_{k \in I}$ , for some index set  $I$ . The catchment basin  $CB(m_i)$  of a minimum  $m_i$  is defined as the set of points  $x \in \mathcal{D}$  which are topographically closer to  $m_i$  than to any other regional minimum  $m_j$ :

$$CB(m_i) = \{x \in \mathcal{D} \mid \forall j \in I \setminus \{i\} : f(m_i) + T_f(x; m_i) < f(m_j) + T_f(x; m_j)\}.$$

The watershed of  $f$  is the set of points which do not belong to any catchment basin:

$$Wshed(f) = \mathcal{D} \cap \left( \bigcup_{i \in I} CB(m_i) \right)^c.$$

Let  $W$  be some label,  $W \notin I$ . The watershed transform of  $f$  is a mapping  $\lambda: \mathcal{D} \rightarrow I \cup \{W\}$ , such that  $\lambda(p) = i$  if  $p \in CB(m_i)$ , and  $\lambda(p) = W$  if  $p \in Wshed(f)$ .

So the watershed transform of  $f$  assigns labels to the points of  $\mathcal{D}$ , such that (i) different catchment basins are uniquely labeled, and (ii) a special label  $W$  is assigned to all points of the watershed of  $f$ . For implementation details and other definitions of the watershed transform we refer the reader to [14]. For real world medical images, meaningful object regions in an image are rarely segmented correctly by the standard watershed transform due to the well known over-segmentation problem resulting from local minima. Meyer et al. proposed a marker-controlled watershed [8] segmentation method to overcome this problem. The marker-based watershed transform [15, 17, 18] is a technique suitable for interactive segmentation. Its properties have been studied in [16] with robustness of the marker placement with being one advantageous property to reduce inter and intra-observer segmentation variability. The watershed transform yields the same results for two different sets of markers as long as they are located within the same catchment basin.

## III. INTERACTIVE SEGMENTATION

Marker locations are used from where the flooding process starts. The physician draws and indicates intuitively the object region (red)  $l(p) = +1, p \in \mathcal{M}$  and background region (green)  $l(p) = -1, p \in \mathcal{M}$  of the GA patches rather than manually labeling or drawing the GA boundaries. Here  $\mathcal{M}$  denotes the domain of the label or marker image  $l$  imposed over  $f$ . The catchment basins of  $f$  are then obtained through the following recursion:

$$X_{h_{min}} = T_{h_{min}}(l)$$

$$X_{h+1} = \min_{h+1} \cup IZ_{T_{h+1}(l)}(X_h); \forall h \in [h_{min}, h_{max}].$$

The next iteration set  $X_{h+1}$  is composed of the union of all regional minima at  $h$  and the union of geodesic influence zones of the connected components of  $X_h$ . To deal with different level of noise and multi-scale edges the expert is able to define the kernel size of the generalized Sobel operator interactively during the labeling process. In the current implementation the kernel size is a mapping of the marker size bounded by the feasible kernel range that is between 3x3 and 9x9. We perform non-linear gradient approximation using generalized separable Sobel kernels [11, 12] for fast edge detection and smoothing. In polynomial transform representation we have

$$H(p, q) = \mathcal{P}_2[f(x, y)] = \sum p^x q^y f(x, y)$$

$$\frac{\partial}{\partial x} \Rightarrow (1+p)^{n-1} (1+q)^n (1-p)$$

$$\frac{\partial}{\partial y} \Rightarrow (1+p)^n (1+q)^{n-1} (1-q),$$

where the generalized Sobel kernels can be computed with  $n \in [1, \dots, 8]$ . The generalized kernels are good approximations of derivatives of Gaussians and are easy to implement. Through

this interactive process the physician obtains direct feedback as object and background markers are drawn approximately onto the image. A schematic overview of the segmentation workflow is shown in figure 2. The approach also supports implicitly the segmentation of multiple classes, however in our application binary class segmentation suffices our needs.

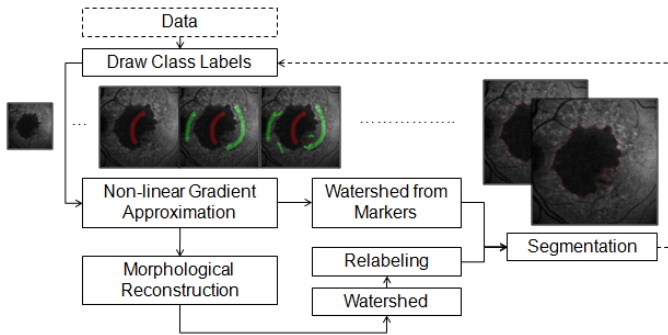


**Fig. 2.** Interactive segmentation workflow for GA segmentation. The process starts with approximate class label information drawn by the expert. Prior to computing the watershed transform non-linear gradient approximations using generalized Sobel kernels are computed. The watershed transform can be either computed from the geodesic reconstructed image or directly using the marker-based watershed transform.

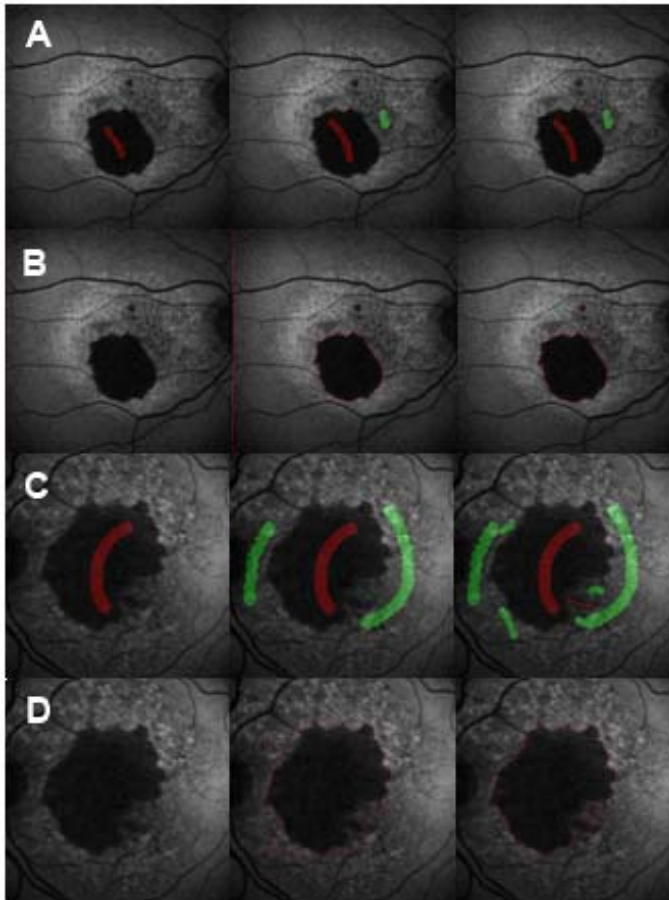


**Fig. 3.** FAF images and example of geographic atrophy (GA). Iterative interactive segmentation process with direct feedback of the segmentation result to the physician. Row A and C show user provided markers through the interactive labeling process. Row B and D show the corresponding segmentation result.

#### IV. EXPERIMENTS AND RESULTS

We have evaluated our interactive segmentation approach on 100 FAF images and compared segmentation performance with the random walker algorithm [5]. An expert provided ground truth information for all 100 FAF images. FAF images had been recorded using the Heidelberg model HRA confocal SLO (Heidelberg Inc, Heidelberg, DE). This instrument uses blue laser light at 488 nm for illumination and a barrier filter at 500 nm to limit the captured light to auto fluorescent structures. The FAF images consisted of bit-mapped laser scans of varying image resolution from 256x256 to 870 x 870 pixels in size, partially centered on the macula and otherwise comprising the whole retina. Each image was an average of 3 to 6 scans composed by the SLO software. All images had a scale of approximately 15 $\mu$ m per pixel. The random walker algorithm was executed with all default parameter values e.g. beta = 90 and implementation was obtained from available source code mentioned in [5]. ROC analysis was performed on a pixel-by-pixel basis with respect to expert gradings and compared for both algorithms. Quantitative evaluation experiments on 100 FAF images show a mean sensitivity / specificity of 98.3 / 97.7% for the watershed transform and a mean sensitivity / specificity of 88.2 / 96.6% for the random walker algorithm.

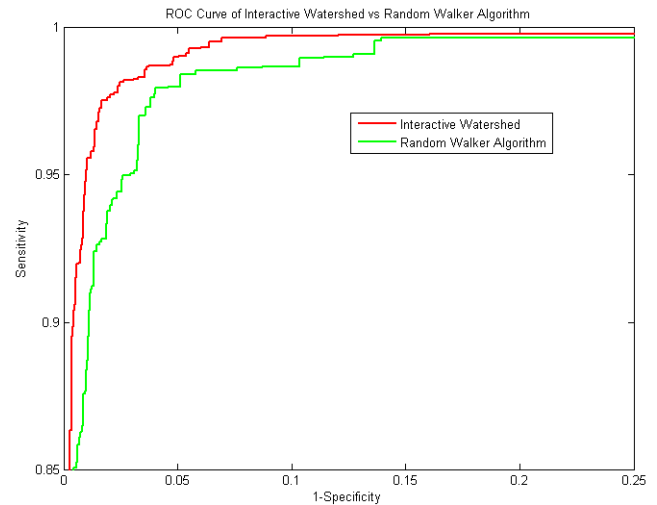


**Fig. 4.** ROC curve for the two interactive segmentation approaches. The upper left curve shows the performance of the watershed approach whereas the lower right curve shows the random walker performance.

TABLE I  
ROC STATISTICS OF INTERACTIVE SEGMENTATION PERFORMANCE FOR WATERSHED TRANSFORM AND RANDOM WALKER ALGORITHM.

ROC Statistic	Watershed Transform	Random Walker
$\mu_{sensitivity}$	<b>98.3%</b>	88.2%
$\mu_{specificity}$	<b>97.7%</b>	96.6%
$\sigma_{sensitivity}$	2.3%	10.8%
$\sigma_{specificity}$	2.1%	8%

The interactive segmentation approach for GA quantification was well perceived from physicians. The watershed approach outperforms the random walker algorithm in terms of sensitivity and specificity. The RW algorithm however has improved noise resistant compared to WT algorithm whereas

WT is more resistant to label placement. The figure below shows qualitative segmentation results of GA obtained with the WT approach.

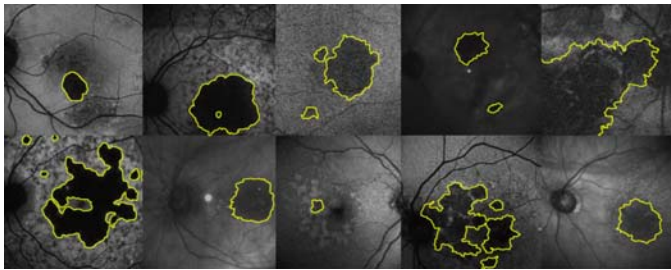


Fig. 5. FAF images and example of geographic atrophy (GA) segmentation.

## V. CONCLUSION

We have presented a simple and intuitive interactive segmentation approach for GA segmentation in FAF images using the watershed transform. We validated our approach with quantitative comparison to the random walker algorithm using ROC statistics. Our approach has potential to perform well for other retinal disorders and application areas for generic object segmentation. The segmentation adaptively iterates to the desired segmentation result that is in conformance to the perception and knowledge of the physician. Furthermore, since only approximate label information is required the labeling process across physicians is more coherent and time efficient than manual labeling. Especially in pathological cases where higher medical expert knowledge is crucial to distinguish similar looking object regions this approach directly integrates expert a priori information which would be hard or even impossible to robustly model mathematically. Future research is intended towards the integration of interaction tools that allow the segmentation of spot like GA manifestations.

## ACKNOWLEDGMENT

This work was funded by NEI (R01 EY015520), the NYC Community Trust (RTS), and unrestricted funds from Research to Prevent Blindness.

## REFERENCES

- [1] Delori F.C., Fleckner M.R., Goger D.G. et al.: *Auto-fluorescence distribution associated with drusen in age-related macular degeneration*. Invest Ophthalmol Vis Sci. (2000); Vol. 41; 496-504.
- [2] Delori F.C., Dorey C.K., Staurengi G. et al.: *In vivo fluorescence of the ocular fundus exhibit its retinal pigment epithelium lipofuscin characteristics*. Invest Ophthalmol Vis Sci. (1995); Vol. 36; 718-29.
- [3] Sunness J.S.: *The natural history of geographic atrophy, the advanced atrophic form of age-related macular degeneration*. Mol Vis. (1999); Vol. 5; 25-9.
- [4] Holz F.G., Bellmann C., Staudt S. et al.: *Fundus auto-fluorescence and development of geo-graphic atrophy in age-related macular degeneration*. Invest Ophthalmol Vis Sci. (2001); Vol. 42; 1051-6.
- [5] Leo Grady: *Random Walks for Image Segmentation*. IEEE Trans. on Pattern Analysis and Machine Intelligence, Vol. 28, No. 11, pp. 1768-1783, Nov., 2006
- [6] Grau V., Mewes A.U.J., Alcaniz M., Kikinis R., Warfield S.K.: *Improved Watershed Transform for Medical Image Segmentation Using Prior Informatio*. IEEE Transactions on Medical Imaging, vol. 23, no. 4, pp. 447-458, April 2004.
- [7] Beucher S. and Lantuejoul C.: *Use of watersheds in contour detection*. Int. Workshop on Image Processing, Real-Time edge and motion detection/estimation. CCETT/INSA/IRISA, IRISA Report, no 132, pp. 2.1-2.12, Rennes, France 17-21 Sept. 1979.
- [8] Meyer F. and Beucher S.: *Morphological Segmentation*. Journal of Visual Communication and Image Representation, vol. 1, no. 1, pp. 21-46, Sept. 1990.
- [9] Hwang J. C., Chan J. W. K., Chang S. et al.: *Predictive Value of Fundus Auto-fluorescence for Development of Geographic Atrophy in Age-Related Macular Degeneration*. Invest Ophthalmol Vis Sci. 2006.
- [10] Deckert A., Schmitz-Valckenberg S., Jorzik J. et al.: *Automated analysis of digital fundus auto-fluorescence images of geographic atrophy in advanced age-related macular degeneration using confocal scanning laser ophthalmoscopy (cSLO)*. BME Ophthalmology. (2005); vol 5.
- [11] Danielsson P.E., Seger O.: *Generalized and separable sobel operators, in Machine Vision – Acquiring and Interpreting the 3D scene* (H. Freeman, ed.), Academic Press, 1986.
- [12] Goekstorp M., Danielsson P.E.: *Velocity tuned generalized sobel operators for multiresolution computation of optical flow*. Image Processing, 1994, Proceedings ICIP, vol. 2, pp. 765-769.
- [13] Bindewald A., Bird A.C., Dandekar S.S. et al.: *Classification of Fundus Auto-fluorescence Patterns in Early Age-Related Macular Disease*. Invest. Ophthal Vis Sci. (2005); Vol. 45; 3309-14.
- [14] Jos B.T.M. Roerdink et al.: *The Watershed Transform: Definitions, Algorithms and Parallelization Strategies*. Fundamenta Informaticae 41(2001) 187-228, IOS Press.
- [15] Rivest, J., Beucher, S., Delhomme, J.: *Marker-controlled segmentation: an application to electrical borehole imaging*. Journal of Electronic Imaging 1(2), pp. 136-142. 1992.
- [16] Lotufo R.A. and Falcao A.X.: *The ordered queue and the optimality of the watershed approaches*. In *Mathematical Morphology and its Application to Image and Signal processing*. pp. 341-350, Palo Alto, USA, June 26-28 2000. Kluwer Academic Publishers.
- [17] F. Meyer: *Minimum spanning forest for morphological segmentation*. In J. Serra and P. Soille, editors, *mathematical Morphology and Its application to image and signal processing*, ISMM'94. Kluwer Academic Publisher, 1994.
- [18] Lotufo R., Silva W.: *Minimal Set of Markers for the Watershed Transform*. Proceedings of ISMM'2002, pp. 359-368. 2002.
- [19] Vincent, L. Soille, P.: *Watersheds in digital spaces: An efficient algorithm based on immersion simulations*. IEEE Transactions on Pattern Analysis and Machine Intelligence 13(6), pp. 583-598. 1991.
- [20] Lee N., Caban J., Ebadollahi S., Laine F.A., *Interactive Segmentation in Multi-Modal Medical Imagery using a Bayesian Transductive Learning Approach*. SPIE Medical Imaging Conference, 2009.
- [21] Lee N., Laine A.F., and Smith T.R., *Coarse to Fine Segmentation of Stargardt Rings using an Expert Guided Dual Ellipse Model* 30th Annual International Conference of the IEEE Engineering in Medicine and Biology Society (EMBC), p. 177, Vancouver, Canada, 2008, 2008.